

Selective Cretaceous Coal Depositional Environment Identification: Perspectives from Organic Petrography, Mineralogy, and Geochemistry

Segun A. Akinyemi^{1,2}, Bemgba B. Nyakuma³, Ayobami T. Kayode¹, Olajide F. Adebayo¹, Henry Y. Madukwe¹, Abiodun B. Ogbesejana⁴, Binoy K. Saikia⁵, James C. Hower^{6,7}

¹ Department of Geology, Faculty of Science, Ekiti State University, P.M.B. 5363, Ado Ekiti, Ekiti State, Nigeria.

² Energy, Environmental & Nanosciences Group, Faculty of Science, Ekiti State University, P.M.B 5363, Ado Ekiti, Ekiti State, Nigeria.

³ Department of Chemical Sciences, Faculty of Science and Computing, North-Eastern University Gombe, P.M.B. 0198 Gombe State, Nigeria.

⁴ Department of Applied Chemistry, Federal University Dutsin-Ma, P.M.B. 5001, Dutsin-Ma, Katsina State, Nigeria.

⁵ Coal & Energy Group, Materials Science & Technology Division, CSIR-North East Institute of Science & Technology, Jorhat, 785006, India.

⁶ Centre for Applied Energy Research, University of Kentucky, 2540 Research Park Drive, Lexington, Kentucky 40511, United States of America.

⁷ Department of Earth & Environmental Sciences, University of Kentucky, Lexington, Kentucky 40506, United States of America

Received June 17, 2024; Accepted September 12, 2024

Abstract

The mineralogy, thermal behaviour, physicochemical characteristics, and organic petrographic composition of Cretaceous coals from the Benue Trough were examined for their quality, paleo-depositional environment, and the factors that control their coal-bearing formations. Seven coal samples were obtained from the Lower, Middle, and Upper Benue Troughs in Nigeria. The samples were examined through X-ray diffraction, Fourier transform-infrared spectroscopy, thermal gravimetry, and organic petrography. Minerals found detected were kaolinite, quartz, feldspar, hematite, magnetite, calcite, siderite, dolomite, orthoclase, graphite, and illite (unknown crystal plane). FTIR spectra confirmed the presence of clay minerals in the samples. Thermal analyses revealed weight loss due to moisture, volatile matter, and fixed carbon contents. The average of high volatile matter yields, low ash yield, high fixed carbon, and low sulphur indicate good quality coal. Vitrinite generally dominated the organic matter, accounting for 52.6 vol.% (mineral-free), with varying inertinite and liptinite contents. Liptinite macerals dominated the Obomkpa (BMK) sample. The analysed coal samples were accumulated in alternating oxic and anoxic moor conditions. DDG and SKJ coal samples were deposited in planar central mires with frequent flooding. OGB and BMK were deposited at the planar mire's lateral edge due to brief submergence. GMG and WKP were deposited in transitional-dry and transitional-wet mires, respectively. AFZ, BMK, DDG, OGB, WKP, and SKJ have high-GI and low TPI deposited in limno-telmatic facies or wet forest swamps with rapid organic matter accumulation. GMG has a low GI and a high TPI, indicating that terrestrial plants contributed significantly rather than microbial organic matter.

Keywords: Cretaceous coals; Benue Trough; Mineralogy; Physicochemistry; Petrology; Depositional environments.

1. Introduction

Coal is a sedimentary rock rich in organic material made of coalified vegetation [1]. The maceral and chemical contents of coal seams, however, differ greatly on both the lateral and vertical axes, indicating that the characteristics of any small number of coals can be taken into account as an accurate depiction of samples [2]. Many studies have examined the petroleum potential of terrestrial coal sediments [3-5].

According to [6-8], the organic matter present in shales (coaly shales) and coal horizons are prospective sources of oil and gas. It may be helpful to forecast the depositional conditions that lead to the formation of coals with high liptinite or per-hydrous vitrinite levels. Most oil-bearing coals are Jurassic-Cenozoic due to the dispersion of such coals in time and space [2]. In addition, the amount of inorganic transition elements in crude oil has a considerable impact on the type of source rock, depositional conditions, and maturity. This is the case because diagenetic or in-reservoir modifications do not affect the ratio of transition elements in petroleum [9-11].

The Benue Trough (BT) and other basins in Nigeria have seen several discoveries of coal and liquid hydrocarbon resources over the years [12-20]. Despite the many findings, the paleo-depositional context that predominated peatification and coalification in the BT coals has received little attention in the literature.

For example, the depositional environment of Cretaceous coals and the coal sequence around the Obi/Lafia portion of the Middle BT in northern Nigeria was described by Obaje [21]. In addition Ogala [22], investigated the paleoenvironments in which lignite from southern Nigeria's Ogwashi-Asaba Formation was deposited. Some authors [20,23] investigated the paleo-depositional environments that influenced a few specific coal-bearing formations in the Lower, Middle, and Upper BT Basins. Due to the absence of specific information on several recently discovered coal deposits in the BT Basin, there are significant chances to examine and comprehend their depositional conditions. The present study seeks to critically analyze the quality and depositional settings of selected Cretaceous coals through combined mineralogy, physicochemistry, thermal gravimetry, and organic petrography approaches.

2. Geology of the study area

The West-Central African basement was split at the start of the Cretaceous period, forming the Nigerian Benue Trough (BT), a linear lithospheric zone. The BT consists of around 6,000 meters of Cretaceous sediment, while earlier sediments were faulted, folded, and occasionally elevated before the mid-Santonian [24]. Geological evidence indicates lakes and rivers deposited sediments that eventually formed the Trough. The BT was likewise created when the Atlantic Ocean was expanding in the early Cretaceous [25]. Geographically, the BT spans 800 km in length and 150 km in width from NNE to SSW [26]. The northernmost edge of the BT is situated south of the boundary with the Chad Basin and the southern border is located at the northern frontier of the Niger Delta (Fig. 1) [27]. A strike-slip system of axial faults, locally developing compression, and tensional regimes actively governed the tectonic evolutions of the BT [25]. Basement horsts and basins were produced due to the subsequent thermal disturbances, lithospheric stresses, and rheology, which either constrained or released some fault-based bends [25,28] proposed a model that focused on the development and end of the mantle upwelling beneath the Cretaceous hot spot. The associated configurations of doming, magmatism, rifting, tectonism, and sedimentation are proposed for the rift zone in the BT. The Lower, Middle, and Upper regions make up the three sections of the BT (Fig. 1). The most significant towns (localities or villages) that make up the centres of the various regions are frequently described in the literature [26,29-30], even though the boundary of the distinct areas is not clearly defined.

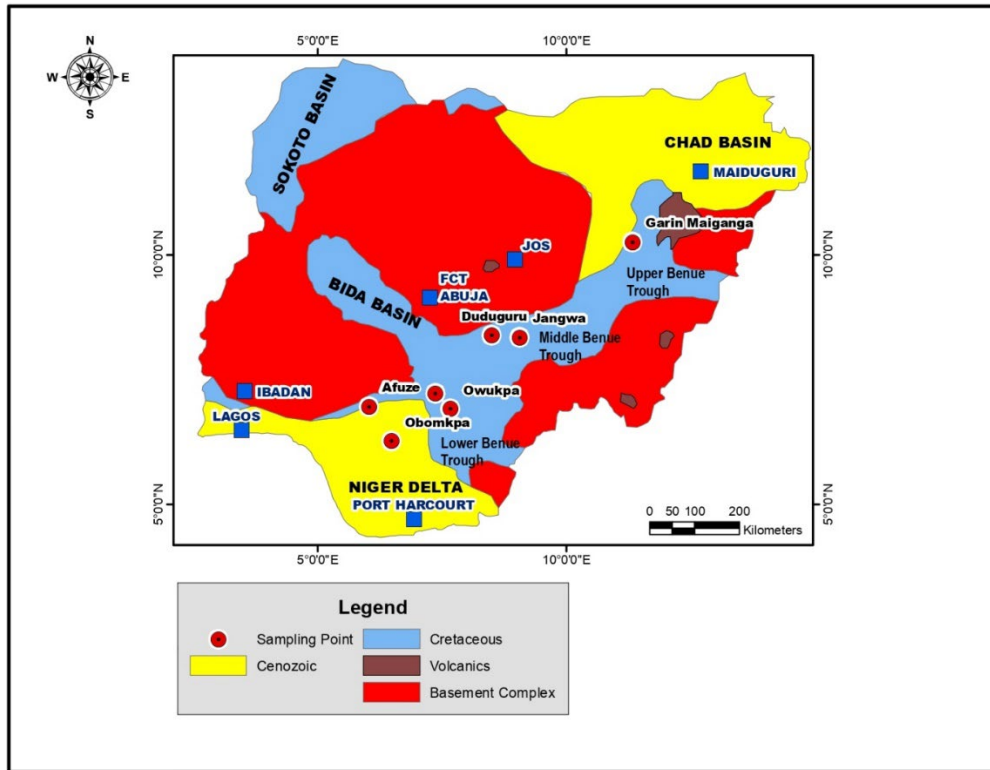


Figure 1. Geological map showing the Benue Trough Basin with inset sampling locations.

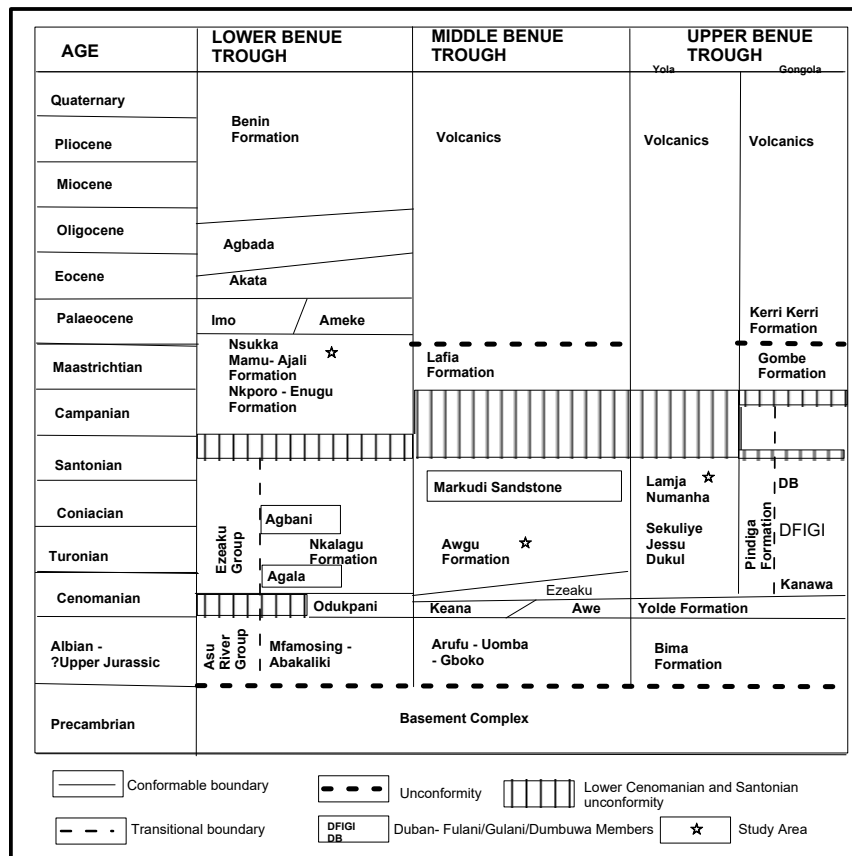


Figure 2. Stratigraphy of the Benue Trough (adapted from [14]).

According to its stratigraphic context (Fig. 2), the maritime Neocomian-Albian Asu River Group and the Lower Benue Trough (LBT) were the two main initiators of sedimentation. However, there aren't many reports about specific pyroclastics from the Aptian to the Early Albian age [31-32]. According to [28], the Asu River Group sediments in the LBT mainly comprise siltstones, isolated sandstones, limestone, and shales. In addition, the deposits consist of extrusive and intrusive residues in the Abakaliki Formation and Mfamosing Limestone in Abakaliki and the Calabar Flank, respectively [26,33-35]. Nigeria's most significant and purest limestone resources (96% CaCO₃) are located in the shallow-water Albian strata near

Mfamosing, which are actively mined for cement manufacturing [36-37]. According to numerous reports, BT and other sedimentary basins in Nigeria have mineral resources with significant commercial potential [27,38]. Barites, clay, glass sand, gypsum, phosphate, limestone, cassiterite, ironstone, manganese, mica, silver, uranium, and, in particular, coal are selected examples [24,38]. Most coals in the BT are non-coking [24,38]. Nonetheless, the coals could be utilised for chemicals, synthetic fuels, fertilizer, or coal-fired electricity production [39-40].

3. Materials and methods

3.1. Coalfield locations and sampling

Samples from the coal mines were obtained using proportionate layered random sampling. To gather new and representative samples, this sampling strategy involves collecting the coal sample fractions in each seam or stratum according to the thickness of the band (lithotype). Each coal sample weighed around 200 g and was placed into a zip-locked polythene bag before being delivered to the laboratory for testing. The labels on the coal samples examined are; AFZ for Afuze coal, BMK for Obomkpa coal, DDG for Duduguru coal, GMG for Garin Maiganga coal, OGB for Ogboligbo coal, SKJ for Shankodi-Jangwa coal, and WKP for Owukpa coal.

3.2. Sample preparation

The coals were prepared according to the ASTM D-2013 standard operating procedures [41]. The samples are cut with a sample riffler before being crushed by a hammer mill to a particle size below 2.36 mm (mesh size 8). The crushed materials were pulverized and sorted into particle sizes below 850 μm (20 mesh) using a plate grinding mill before petrographic investigation. The leftover material was recrushed in a pulveriser and then sieved into particles below 250 microns (mesh size: 60) for laboratory analyses.

3.3. Laboratory analytical techniques

The collected coal samples were investigated through X-ray diffraction analysis (XRD) and Fourier transform infrared spectroscopy (FTIR) to examine their chemical properties and bulk mineralogy, respectively. The physicochemical studies determined the proximate, ultimate, and calorific values, whereas organic petrographic analysis examined maceral composition. Sections 3.2.1 through 3.2.5 illustrate the detailed procedures.

3.3.1. X-ray diffraction

The pulverised coal samples were examined using an X-ray diffractometer (Rigako Ultima IV) at a voltage of 40 kV, current of 40 mA, and power of 1.6 kW. The XRD data were collected using the target Cu-K ($\lambda = 1.5406\text{\AA}$) based on the following parameters: 2.00 as the beginning angle, 90.00 as the stopping angle, and 0.02 as the step angle. Peaks were identified using the Rigaku PDXL 1.2.0.1 library database connected to the apparatus.

3.3.2. FTIR analysis

Using an FTIR spectrophotometer (System-2000, Perkin-Elmer), FTIR spectra of the coal samples were captured in transmittance mode at 4 cm⁻¹ spectral resolution. Potassium bromide (KBr) powder was used to create sample pellets using a hydraulic pellet press.

3.3.3. Physicochemical analysis

Thermal gravimetric analysis (TGA Model: LECO, USA) was used to assess the coal's proximal properties including moisture, volatile matter, ash, and fixed carbon. The analyses were performed according to ASTM D7582-12 [42] norms. According to the ASTM D4239-12 standard [43], the LECO carbon/sulfur analyzer completed the total carbon and sulfur analyses. According to the ASTM D3176-15 test protocol, the final analysis (C, H, N, S, and O) was determined on the LECO CHN analyzer [44]. Each test was run three times.

3.3.4. Thermal gravimetric analysis (TGA)

Thermal analysis was conducted using a thermal analyzer (LECO TGA 701 Thermal gravimetric analyzer) in a nitrogen atmosphere at a heating rate of $10^{\circ}\text{C min}^{-1}$ from room temperature to 900°C using an Al_2O_3 crucible.

3.3.5. Organic petrography

The Leitz Orthoplan Microscope (USA), equipped with an oil immersion objective and reflected light (magnification $50\times$), was used to examine the petrologic analysis of the coal samples. Each sample was prepared as an epoxy-bound particle pellet with a final alumina polish of 0.05 microns following ISO 7404-2 [45]. Based on ASTM D7708-14 [46], the composition of the scattered organic matter in the coal samples was determined. The reports on the maceral compositions are presented using nomenclature from Pickel *et al.* [47] and the ICCP [48-49]. Without combining the low-rank and bituminous nomenclature specified in Skorová *et al.* [50], the entire coal count for vitrinites conforms to the ICCP [48]. The vitrinite reflectance was measured using photometer equipment following ISO 7404-5 [51] standard. According to ISO 7404-5 [51], the vitrinite reflectance was measured using a photometer system and polarized light that was incident at a 45° angle and passed through a 546 nm grating.

4. Results and discussion

4.1. Coal mineralogy

According to the diffraction pattern (Fig. 3), samples B-1 to B-7 (i.e., AFZ, DDG, BMK, OGB, GMG, SKJ, and WKP) contain minerals with various crystal planes. Minerals found in the samples were mainly kaolinite (001, 020, 110, -223), quartz (101, 110, 102, 103, 211), feldspar (-202, -222, -422), hematite (104, 110, 006, 116), magnetite (440), calcite (012, 104, 300), siderite (012, 113, 125), dolomite (12-4), orthoclase (-201), graphite (110), and illite (unknown crystal plane).

4.2. FTIR analysis

The broad absorption band at 3434 cm^{-1} , caused by N-H and O-H groups, can be seen in the FT-IR spectra (Fig. 4). Other O-containing functional groups, such as phenols and alcohols, ethers, carboxylic acids, and carbonyls, may also be responsible for the sharp peaks of medium intensity at 2923 cm^{-1} and 2852 cm^{-1} . A prominent band at 1460 cm^{-1} may be due to bridges comprising the CH_2 group and asymmetric CH_3 deformation. The clay minerals [52] observed in the XRD spectra are primarily represented by the peaks between 1100 and 400 cm^{-1} in the FTIR spectra of coals.

4.3. Thermal analysis

The TGA graph depicts the change in weight due to sequential losses of moisture (0 – 130°C), volatile matter (130 – 400°C), and fixed carbon (400 – 800°C) combustion (Fig. 5). At about 800°C , the highest mass loss of up to 75% occurred; after that, no more weight loss was observed in the thermogram. This observation indicates that ash and other inorganic materials make up the residual mass. Fig. 5. TGA graph of the samples demonstrating percentage weight loss at three distinct intervals with temperature increase.

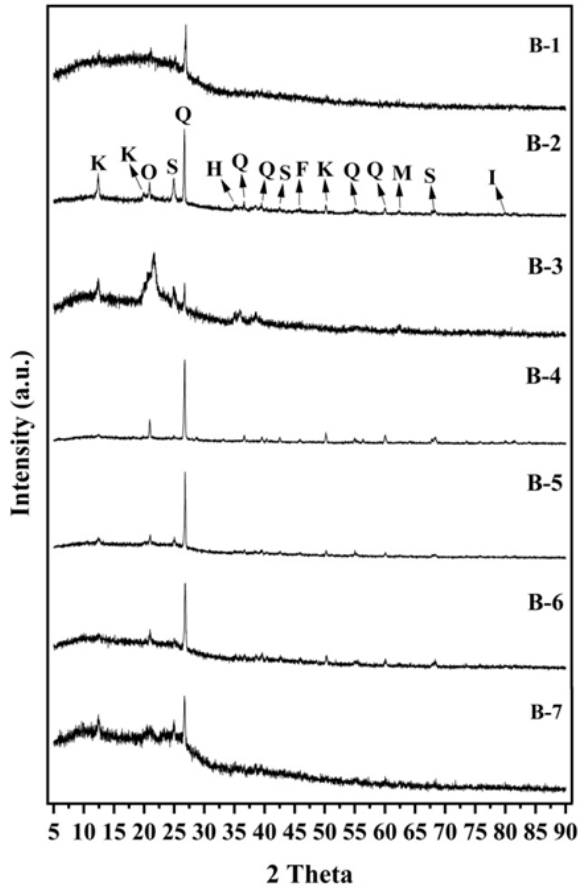


Figure 3. X-ray diffraction patterns of samples B-1 to B-7 (K = Kaolinite, F= Feldspar, Q = Quartz, H = Haematite, M= Magnetite, O = Orthoclase, S=Siderite, C = Calcite, D = Dolomite, I = Illite, and G = Graphite).

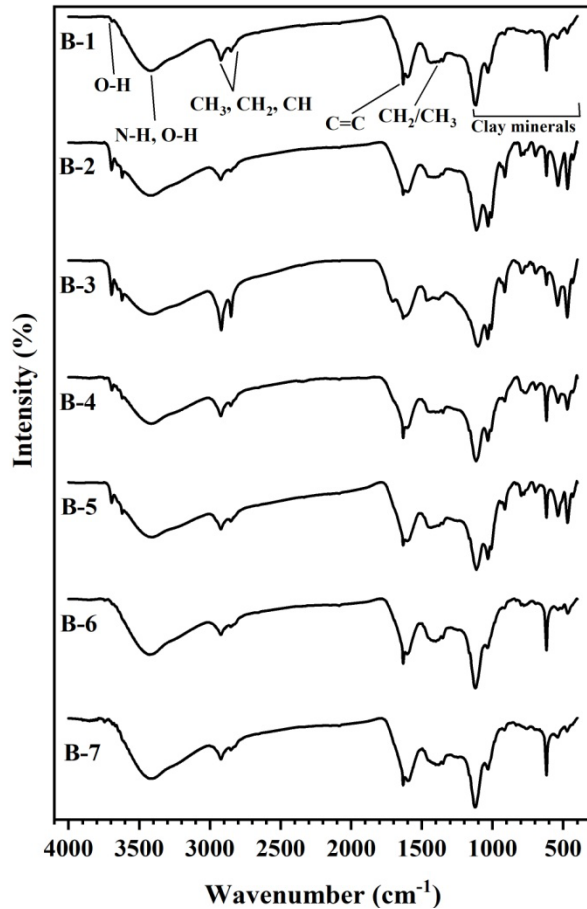


Figure 4. FTIR spectra of the samples exhibiting absorption peaks caused by the presence of functional groups and clay minerals.

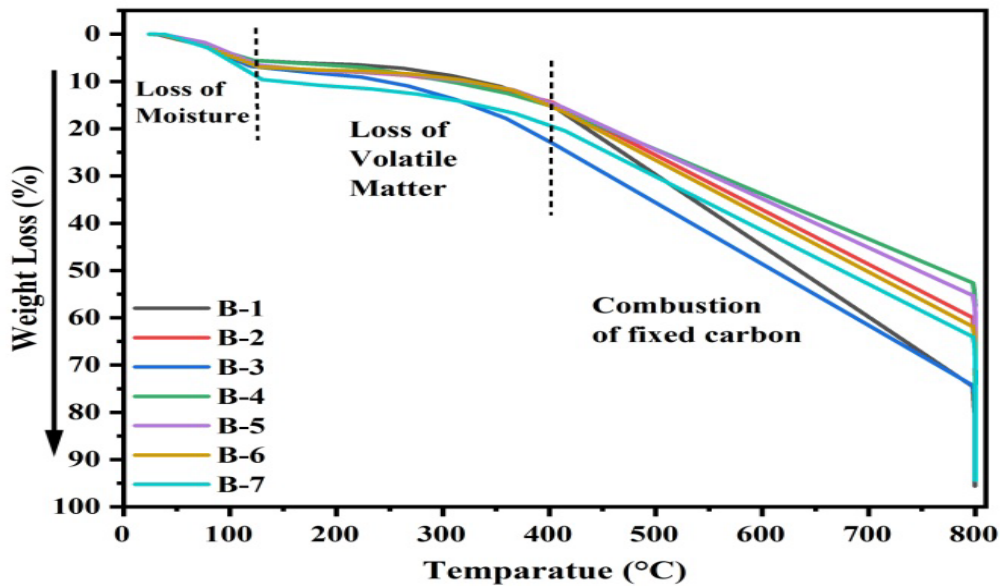


Fig. 5. TGA graph of the samples demonstrating percentage weight loss at three distinct intervals with temperature increase.

4.4. Coal facies

The results of the organic petrography are shown in Table 1 and Figs. 6–11, while Table 2 shows the findings of the proximate and ultimate analyses.

Table 1. Results of organic petrographic analysis. The first column lists the entire amount of minerals, but the second column normalizes the mineral content without including minerals.

Macerals	AFZ		BMK		DDG		GMG		OGB		SKJ		WKP	
Telinite	3.9	3.9	0.0	0.0	10.1	10.5	7.9	8.0	2.3	6.5	6.7	6.9	11.8	12.1
Collotelinite	7.8	7.9	2.4	3.2	18.3	19.0	7.9	8.0	0.4	1.1	4.6	4.7	1.2	1.2
<i>Total telovitrinite</i>	11.6	11.8	2.4	3.2	28.4	29.4	15.8	16.0	2.7	7.5	11.2	11.6	12.9	13.4
Vitrodetrinite	40.3	40.9	10.3	13.7	33.1	34.3	17.9	18.1	12.4	34.4	44.9	46.5	31.8	32.8
Collodetrinite	0.0	0.0	0.0	0.0	0.0	0.0	0.0	0.0	0.0	0.0	0.0	0.0	0.0	0.0
<i>Total detrovitrinite</i>	40.3	40.9	10.3	13.7	33.1	34.3	17.9	18.1	12.4	34.4	44.9	46.5	31.8	32.8
Corropogelinite	6.6	6.7	0.0	0.0	14.8	15.3	8.2	8.3	3.5	9.7	4.9	5.1	9.4	9.7
Gelinite	0.0	0.0	0.0	0.0	0.0	0.0	0.0	0.0	0.0	0.0	0.0	0.0	0.0	0.0
<i>Total gelovitrinite</i>	6.6	6.7	0.0	0.0	14.8	15.3	8.2	8.3	3.5	9.7	4.9	5.1	9.4	9.7
<i>Total vitrinite</i>	58.5	59.4	12.7	16.8	76.3	79.0	41.9	42.4	18.6	51.6	61.1	63.3	54.1	55.9
Fusinite	8.5	8.7	1.6	2.1	5.4	5.6	27.1	27.4	6.2	17.2	6.7	6.9	15.3	15.8
Semifusinite	3.9	3.9	5.6	7.4	3.1	3.2	13.7	13.9	3.5	9.7	3.5	3.6	12.9	13.4
Micrinite	1.9	2.0	0.8	1.1	0.8	0.8	10.0	10.1	0.0	0.0	1.8	1.8	2.0	2.0
Macrinite	0.4	0.4	0.0	0.0	0.0	0.0	0.3	0.3	0.4	1.1	0.4	0.4	1.2	1.2
Secretinite	0.0	0.0	0.0	0.0	0.0	0.0	0.0	0.0	0.0	0.0	0.0	0.0	0.0	0.0
Funginite	0.0	0.0	0.0	0.0	1.6	1.6	0.0	0.0	0.4	1.1	1.1	1.1	0.8	0.8
Inertodetrinite	0.8	0.8	1.6	2.1	0.0	0.0	0.7	0.7	0.0	0.0	0.0	0.0	0.4	0.4
<i>Total inertinite</i>	15.5	15.7	9.5	12.6	10.9	11.3	51.9	52.4	10.5	29.0	13.3	13.8	32.5	33.6
Sporinite	9.7	9.8	1.6	2.1	0.8	0.8	1.0	1.0	0.4	1.1	3.2	3.3	4.7	4.9
Cutininite	2.3	2.4	7.1	9.5	1.9	2.0	1.0	1.0	0.4	1.1	2.1	2.2	3.9	4.0
Resinite	8.1	8.3	4.0	5.3	4.7	4.8	2.7	2.8	5.4	15.1	15.4	16.0	0.0	0.0
Alginite	0.4	0.4	0.8	1.1	0.0	0.0	0.0	0.0	0.4	1.1	0.0	0.0	0.0	0.0
Liptodetrinite	2.3	2.4	38.9	51.6	1.6	1.6	0.0	0.0	0.4	1.1	1.1	1.1	0.8	0.8
Suberinite	1.6	1.6	0.8	1.1	0.4	0.4	0.3	0.3	0.0	0.0	0.4	0.4	0.8	0.8
Esudatinite	0.0	0.0	0.0	0.0	0.0	0.0	0.0	0.0	0.0	0.0	0.0	0.0	0.0	0.0
<i>Total lipinite</i>	24.4	24.8	53.2	70.5	9.3	9.7	5.2	5.2	7.0	19.4	22.1	22.9	10.2	10.5
Silicate	1.6		23.0		3.5		0.7		54.3		1.8		3.1	
Sulfide	0.0		0.0		0.0		0.0		3.5		1.4		0.0	
Carbonate	0.0		1.6		0.0		0.0		0.0		0.4		0.0	
Other	0.0		0.0		0.0		0.3		6.2		0.0		0.0	
<i>Total mineral</i>	1.6		24.6		3.5		1.0		64.0		3.5		3.1	
Rmax	0.44		0.45		0.63		0.46		0.55		0.47		0.53	
Stdev.	0.03		0.03		0.04		0.03		0.03		0.02		0.07	
Rrandom	0.42		0.41		0.61		0.44		0.52		0.44		0.51	
Stdev.	0.03		0.02		0.04		0.02		0.04		0.02		0.08	

Table 2. Results of proximate and ultimate analyses H = Hydrogen, O = Oxygen, C = Carbon, TS = Total Sulphur, N = Nitrogen, TPI = Tissue preservation index, GI = Gelification index.

Sample	AFZ	BMK	DDG	GMG	OGB	SKJ	WKP
Ash %	4.36	25.36	16.99	7.49	49.03	5.71	5.93
M %	2.5	4.17	3.89	8.04	2.52	6.26	6.55
C %	74.47	49.19	60.52	61.67	33.83	66.26	68.02
H %	5.87	5.37	4.78	4.37	3.16	5.69	5.11
N %	1.6	0.64	1.33	1.02	0.8	1.2	1.54
TS%	1.57	2.03	0.77	0.37	3.13	2.47	0.62
O %	12.13	17.41	15.61	25.08	10.77	18.67	18.78
VM %	47.76	48.72	38.81	40.81	27.35	52.6	41.16
FC %	45.38	21.75	40.31	43.66	21.1	35.43	46.36
Aver.	21.74	19.40	20.33	21.39	16.85	21.59	21.56
H/C	0.08	0.11	0.08	0.07	0.09	0.09	0.08
O/C	0.16	0.35	0.26	0.41	0.32	0.28	0.28
C/N	46.54	76.86	45.50	60.46	42.29	55.22	44.17
TS/C	0.02	0.04	0.01	0.01	0.09	0.04	0.01
IV factor	21	43	13	55	36	18	38
TPI	0.48	0.76	0.76	1.53	0.76	0.41	0.92
GI	3.88	1.35	8.17	0.82	1.96	5.13	1.81

According to [53], coal's mineral composition can be used to decipher the depositional environment (Fig. 12). The model makes it possible to comprehend how the ratio of subsidence differs in wet and dry territories. The coals AFZ, DDG, GMG, SKJ, and WKP were accumulated in alternating oxic and anoxic moor environments (Fig. 12). According to [54], this may be related to ocean level changes and eustatic settlement. BMK and OGB, on the other hand, were deposited in moist moors that frequently experienced moderate to high floods, which resulted in a more significant influx of mineral materials. The illustration in Figure 13 provided by Misiak [55] highlights the significance of water levels in coal production. The peat bog's

water surface affects the presence of maceral components. According to Misiak [56], the long-term stages of the mire's flooding and drying needed gradual changes for the plant community.

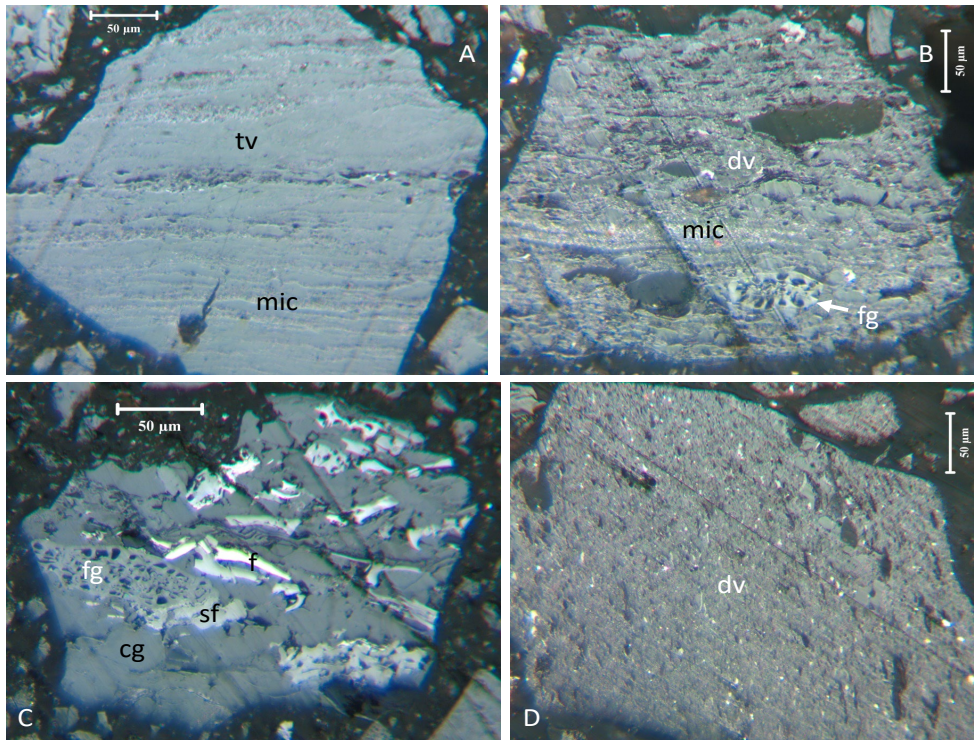


Fig. 6. Vitrinite. (A) Telovitrinite (tv) and micrinite (mic) bands (Image DDG) (B) Detrovitrinite (dv) with resinite (r), funginite (fg), and micrinite (mic) (Image AFZ) (C) Corpogelinite (cg), fusinite (f), semifusinite (sf), and funginite (fg) (Image DDG) (D) Detrovitrinite (dv) (Image SKJ).

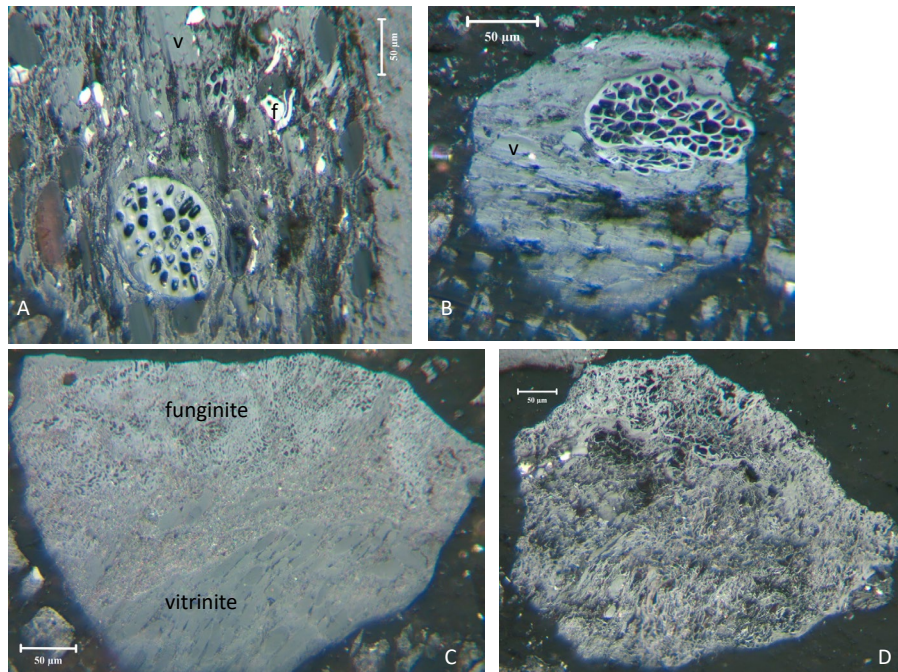


Figure 7. Funginite. (A) Fungal sclerotia with vitrinite (v), fusinite (f), and resinite (r) (Image AFZ) (B) Fungal sclerotia with vitrinite (v) (Image DDG) (C) Funginite with vitrinite (v) (Image SKJ) (D) Funginite (Image WKP).

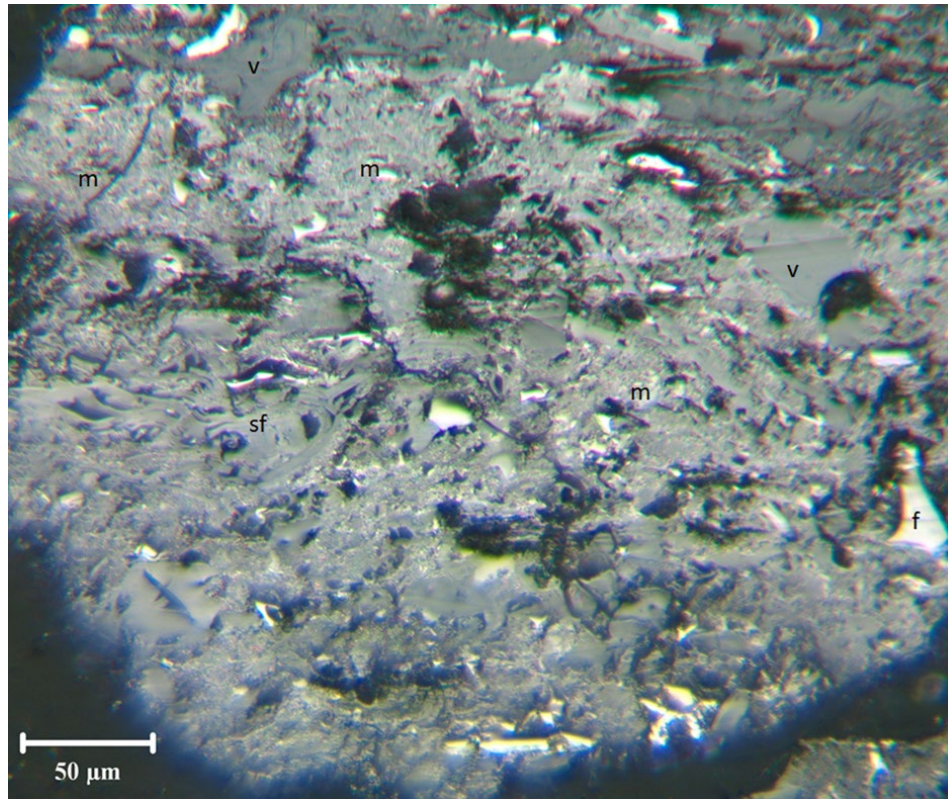


Figure 8. Macrinite (m) with fusinite (f), semifusinite (sf), and vitrinite (Image WKP).

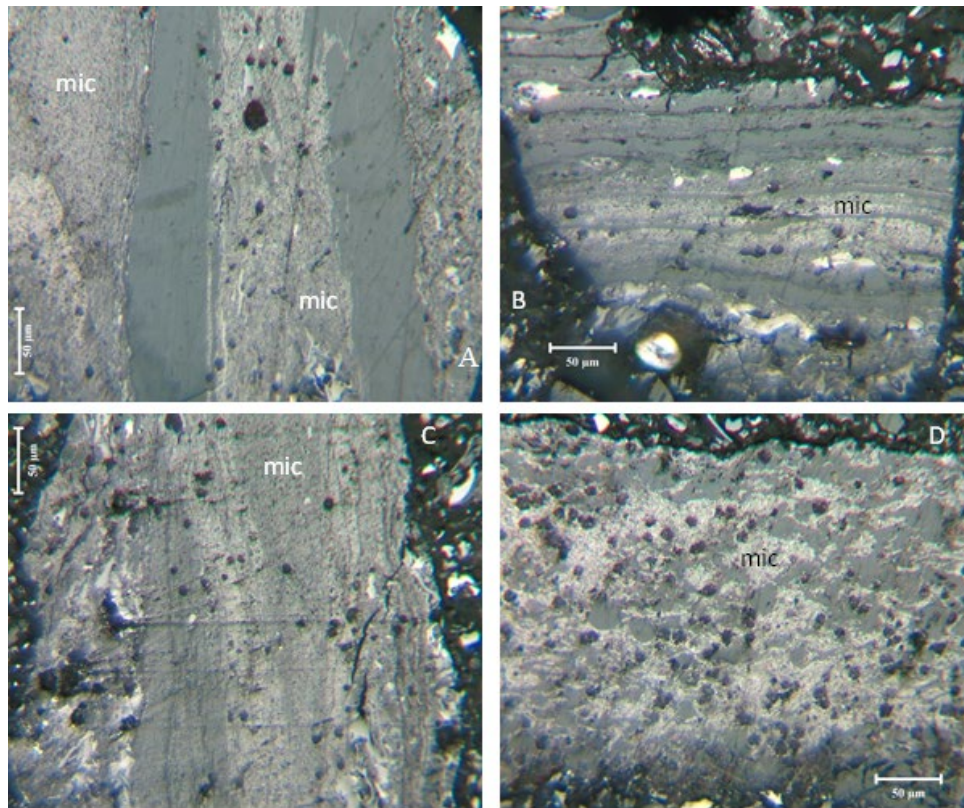


Figure 9. Micrinite (mic) (A) Image GMG 02 (B) Image GMG 03 (C) Image GMG 06 (D) Image GMG 09.

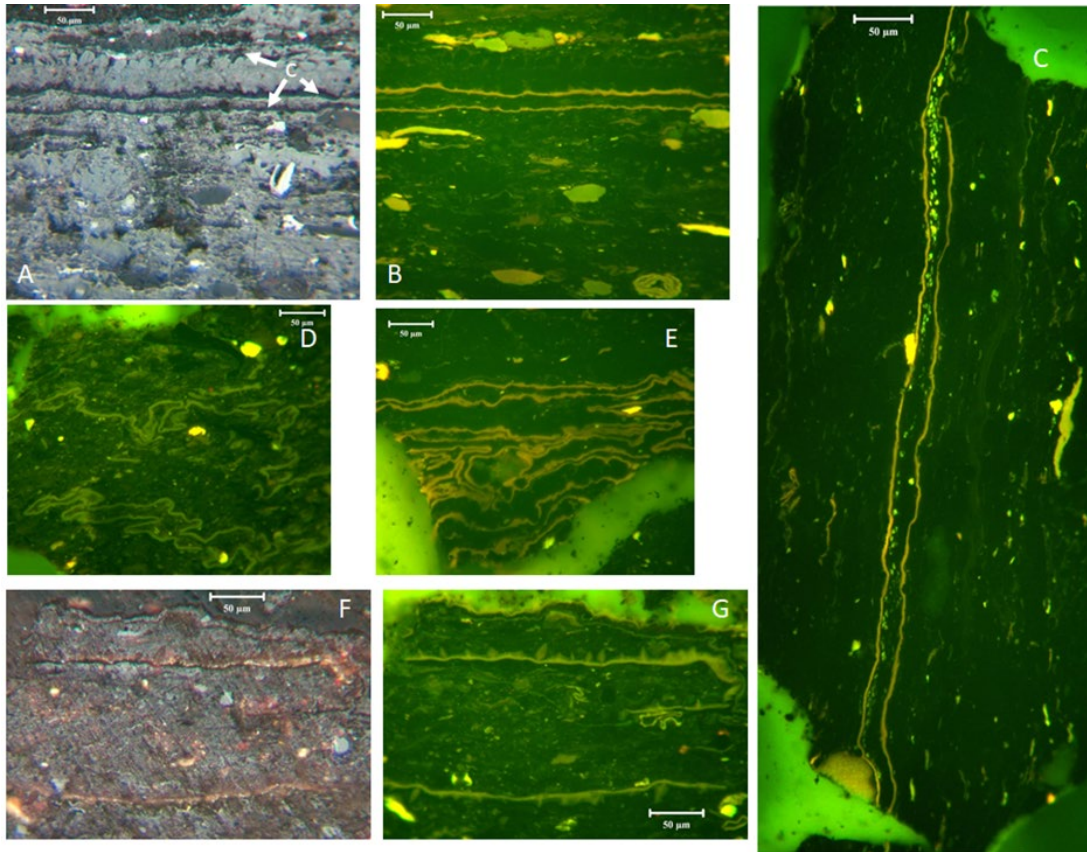


Figure 10. Cutinite (A) White-light images of cutinite (c) in vitrinite (B) blue-light images of cutinite (c) in vitrinite (Image AFZ 07) (C) Blue-light image of cutinite with resinite between cutinite leaves (Image WKP 08) (D) Blue-light image of cutinite (Image BMK 02) (E) Blue-light image of cutinite (Image WKP 06) (F) White-light images of cutinite with vitrinite & (G) blue-light images of cutinite with vitrinite. Note the papillate surface texture on cutinite (Image BMK 05).

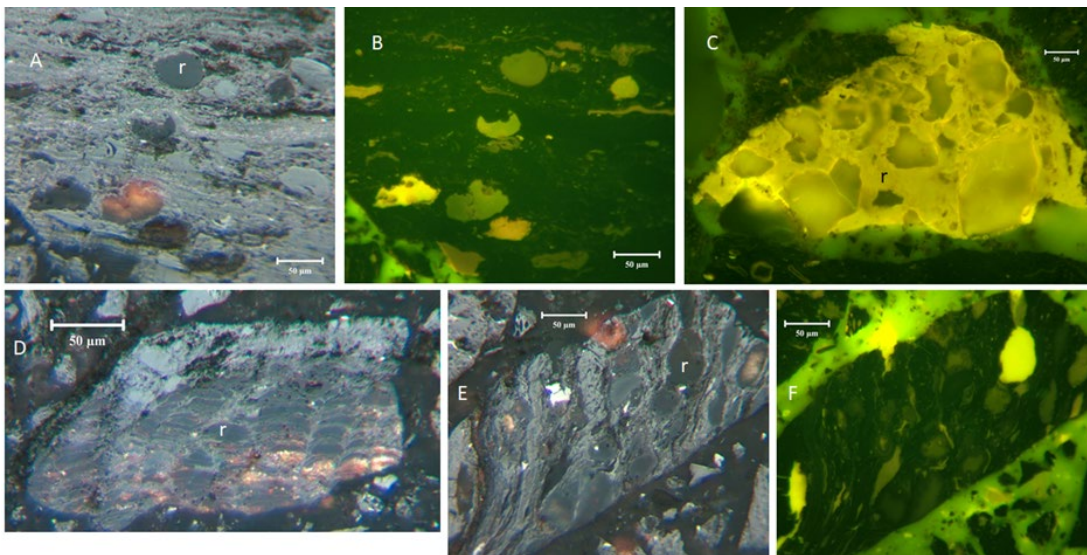


Figure 11. Resinite (A) White-light images of resinite (r) in vitrinite (B) blue-light images of resinite (r) in vitrinite. (Image AFZ 06) (C) Resinite (r) (Image BMK 04) (D) Resinite (r) (Image DDG 15) (E) White-light images of resinite (r) in vitrinite (Image SKJ 08) & (F) blue-light images of resinite (r) in vitrinite (Image SKJ 08).

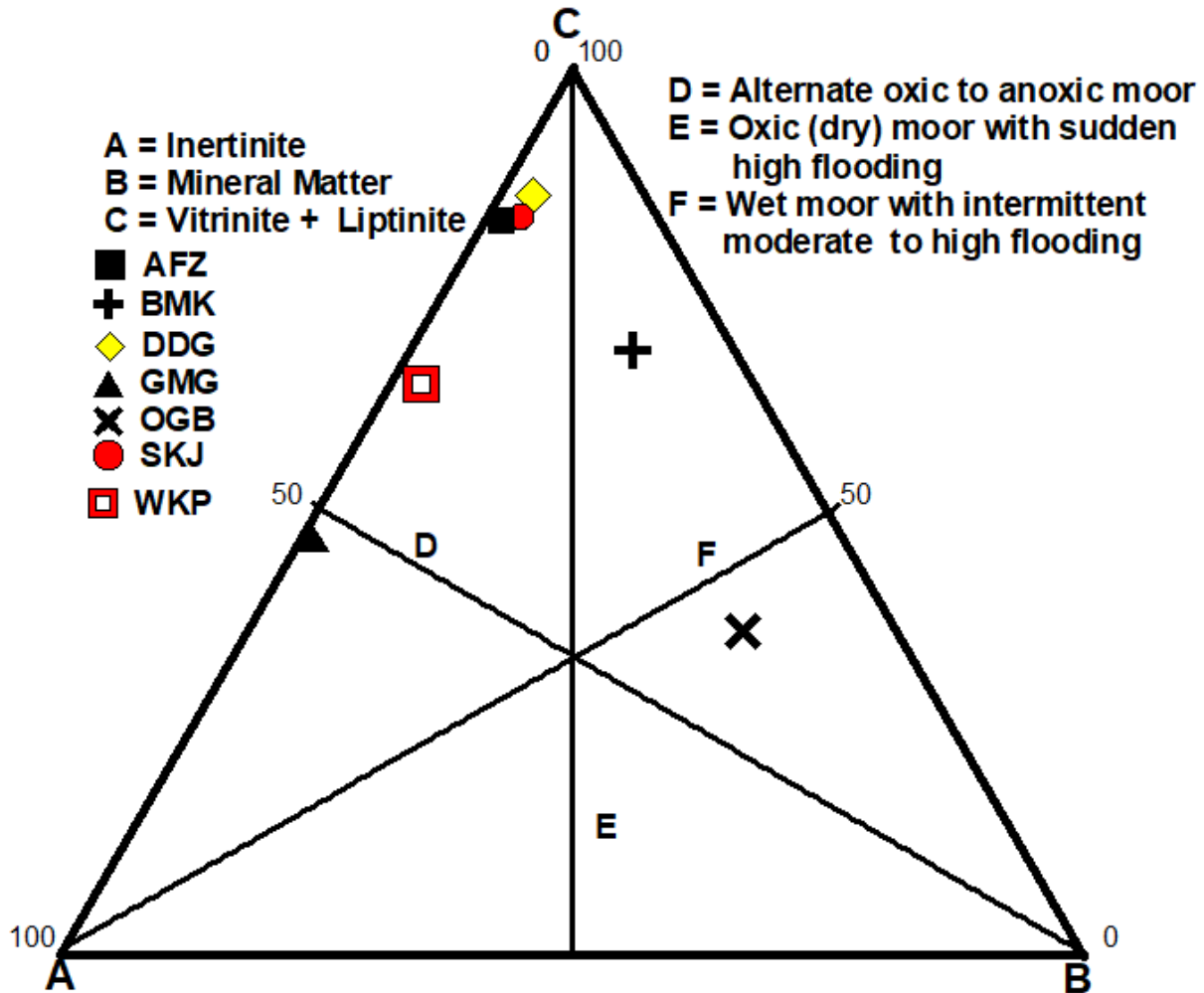


Fig. 12. Depositional condition of the coals studied based on maceral and mineral matter (Adapted from Singh and Singh [54]).

		I ≤ 25%	I > 25%	V > 25%	V ≤ 25%		
		I ≤ 25%	V ≥ I		V < I		
		L ≥ 25%	L < 25%			L ≥ 25%	
		DEM ≥ 10%	DEM < 10%				
WATER TABLE/ PEAT SURFACE		Water table (X +)	(◇ ●)	(□)	(▲)	peat surface	
DEPOSITIONAL ENVIRONMENT	NAME	planar margin mire	planar central mire	transitional-wet mire	transitional-dry mire	Domed progressive mire	Domed regressive mire
		Planar mire 'PM' (permanently inundated)		Transitional mire 'TM' (temporarily inundated)		Domed mire 'DM' (Elevated)	
	SYMBOL	PM 'margin (lake or river)	PM 'central'	TM 'wet'	TM 'dry'	DM 'progr'	DM 'regr'

■ AFZ
+ BMK
◇ DDG
▲ GMG
× OGB
● SKJ
□ WKP

Figure 13. Sedimentary environments of the coals studied, modified from Misiak [56]. DEM = detrital matter, I = inertinite, L = liptinite, V = vitrinite.

In contrast to DDG and SKJ, which were deposited in planar central mires (also constantly inundated), the coals from OGB and BMK were deposited in the planar margin mire. Although temporarily flooded, the GMG and WKP coals were placed in transitional-dry mires and transitional-wet mires, respectively. The GMG and WKP coals' high inertinite percentages (51.9% and 32.5%, respectively) and propensity for more mires suggest drier conditions. The composition of macerals suggests that this process occurs within the ecological amplitude of a certain plant assemblage and causes only minor changes. Misiak [56] contends that the relatively fast oscillations in the water level do not always compel the succession of plants. The inorganic materials associated with organic molecules, dissolved salts in the pore water, and discrete crystalline/non-crystalline particles are all examples of mineral matter in coal [57]. According to [58], Figure 14 demonstrates the importance of the mineral matter composition in coal. High water content intensifies the gelification process, as indicated by the high vitrinite composition. According to this observation, the mineral matter was deposited in basins susceptible to disintegration in the flooded mire, whereas higher inertinites show low water levels [59].

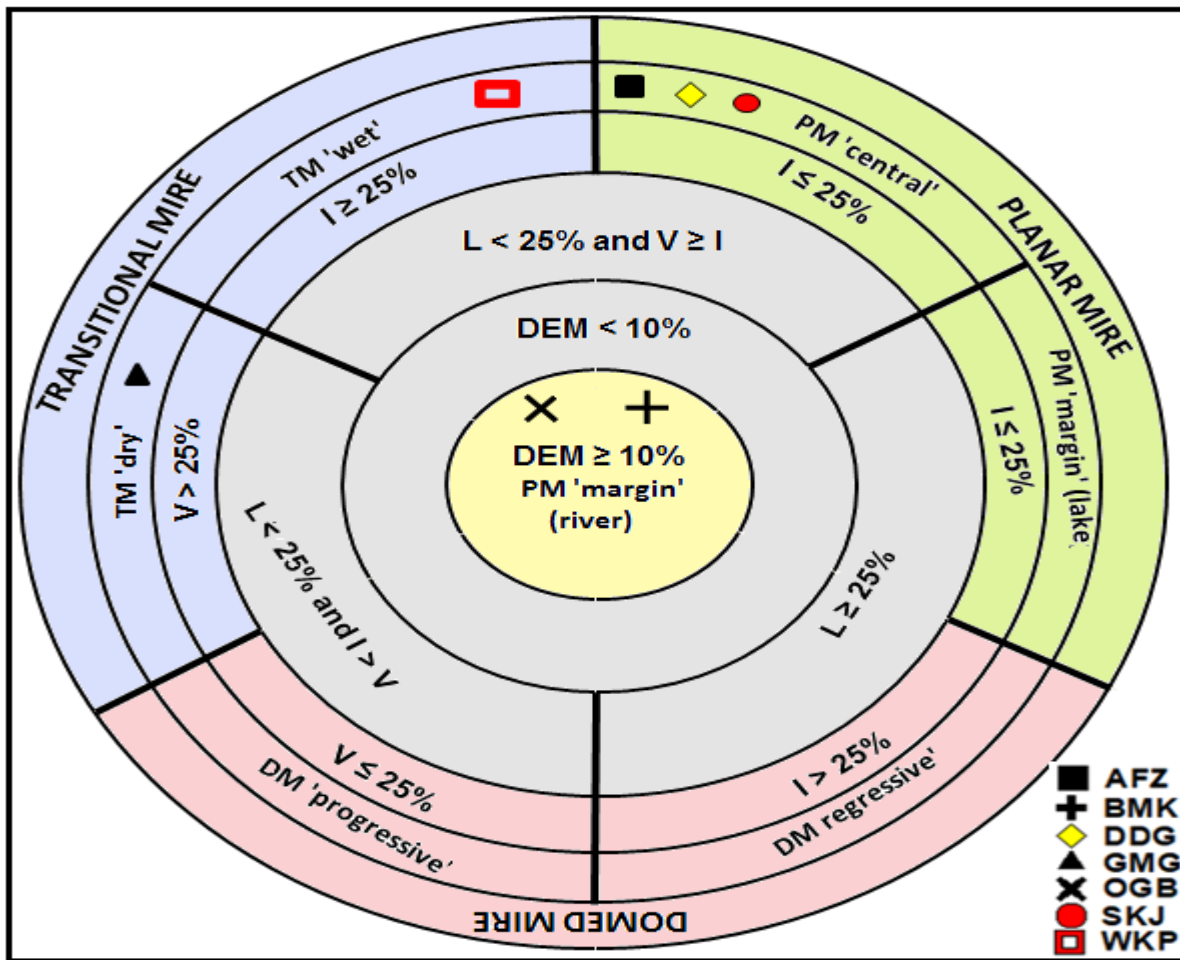


Fig. 14. Diagram of the coal facies analysis of the coals studied, adapted from [58]. DEM = detrital matter, I = inertinite, L = liptinite, V = vitrinite.

Mineral content below 5% is typically associated with tissue degradation, while mineral above 5% indicates that water has entered the mire. Fluvial systems are associated with mineral matter contents significantly higher than 10% [56]. Mineral matter concentrations above 10% in the coals from the OGB and BMK indicate tissue disintegration. In comparison, concentrations below or equal to 25% in AFZ, DDG, and SKJ and above or equal to 25% in

WKP and GMG indicate lacustrine deposits. The peats were created in low-lying marshes, whereas the coal deposits in the BT are autochthonous.

Warbrooke [60] created the concept of coal facies by fusing maceral research with coal ash geochemistry. Warbrooke [61] used two criteria to describe the depositional conditions, using the well-known depositional setting of Hunter Valley coals as an example.

$$IV_{factor} = \frac{Inertinite}{Inertinite + Vitrinite} \times 100 \quad (1)$$

$$SAL_{factor} = \frac{SiO_2}{SiO_2 + Al_2O_3} \times 100 \quad (2)$$

According to the standards outlined by [60], the AFZ, DDG, and SKJ coals were dumped in swampy, wet woodland. However, the BMK, OGB, WKP, and GMG coals were deposited in a swampy, dry, or damp forest. However, caution should be exercised when applying the criteria above because inertinite and vitrinite contain various tangentially related and unrelated substances [61]. Diessel [62] proposed two coal facies indices, tissue preservation index (TPI) and gelification index (GI), with the warning that his formulas were initially intended for the Permian Gondwana coals (see a critique of maceral indices [63]).

$$TPI = \frac{Telovitrinite + Telo - inertinite}{Detro + Gelovitrinite + Detro + Gelo - inertinite} \quad (3)$$

$$GI = \frac{Vitrinite + Gelo + inertinite}{Telo - inertinite + Detro + inertinite} \quad (4)$$

The TPI emphasizes tissue preservation versus destruction, whereas the GI measures the proportion of qualified with fusinitized macerals. Due to the ratio of vitrinite to inertinite, the GI accurately reveals the oxidation state of tissues and indicates the relative water level during peat formation [64]. While a low GI suggests a regressive setting, high GI values indicate high water levels and a transgressive environment. More terrestrial plants should be added than microbial organic matter, as indicated by TPI values above 1 [65].

According to previous authors [66-67], the vegetation is derived from detrovitrinite and herbaceous plants because the TPI values decrease with decreasing tree density. High TPI and GI indices represent the moist conditions during peat production, while low TPI and GI indices represent the dry conditions. Low levels of aerobic breakdown are indicated by a high (>1) TPI and GI combination. However, restricted aerobic decomposition or high levels of anaerobic decomposition are the causes of low TPI and high GI indices. When organic matter builds up quickly, the oxidation stages are kept to a minimum, which leads to high GI and, generally speaking, high TPI. When organic matter builds up quickly, the oxidation stages are kept to a minimum, which leads to high GI and, generally speaking, high TPI.

Figure 15 demonstrates that the high GI and low TPI values of AFZ, BMK, DDG, OGB, WKP, and SKJ were laid down in limno-telmatic facies or wet forest swamps with rapid organic matter accumulation. Conversely, GMG has a low GI and a high TPI, indicating more terrestrial plants were added than microbial organic matter. In essence, underground fungal networks are essential for the growth of trees [68].

These traits point to a weak humification and strong gelification of plant tissues, both caused by significant subsidence rates. Bright (vitrain) to banded bright (clarain) coal types containing telovitrinite generated from wood and bark are present [69]. The GMG occurs in terrestrial facies in a swampy dry forest, and the coal is a wood-derived telo-inertinite, that is banded dull (clarodurain) in colour [69]. While most commercial coal deposits are considered autochthonous, two main types of peat are frequently distinguished: allochthonous and autochthonous [67].

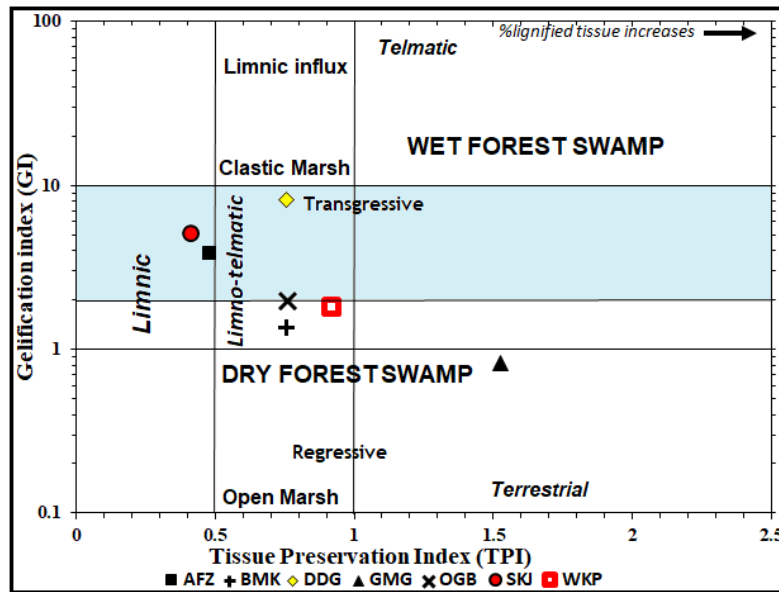


Fig. 15. Facies diagram to identify paleodepositional peat-forming environments of the studied coals (adapted from [62,70]).

4.5. Organic matter type and potential for generating hydrocarbons

The percentage composition of the various maceral kinds in the studied coals is shown in Table 1. Except for GMG, which has more inertinites than vitrinites, all other coal samples have the highest compositions of vitrinite (Type III), followed by the inertinite group (Type IV). As a result, the coals could produce gas at maturity. The maceral makeup of the coals tested in this study, except for BMK, shows a preference for vitric coals (Fig. 16).

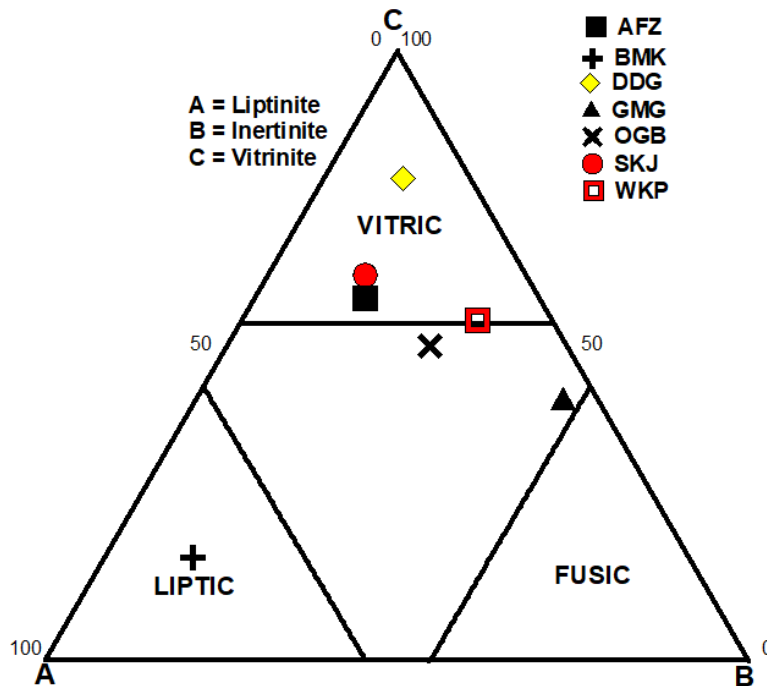


Fig. 16. Maceral groups in the coals studied, after [71].

To distinguish between the aquatic (algal) and terrestrial (land-plant) backgrounds of deposited organic matter, the atomic ratio of carbon to nitrogen (C/N ratio) derived from elemental analyses is frequently used [72-76].

Although vascular land plants have values above 20, lacustrine algae typically have C/N ratios below 10 [77-78]. Higher C/N ratios in river sediments suggest that organic matter from land plants predominates. The C/N ratios of the investigated coals show the presence of organic matter from terrestrial plants is not oil-prone (Table 2). Although planktonic organisms have an N/C ratio > 0.08 for a H/C ratio ranging from 1.3 to 1.5, terrestrial plants typically have an N/C ratio below 0.05 for a H/C ratio around 1.0 [79]. The coals in this study exhibited N/C ratios between 0.01 and 0.02, indicating a terrestrial origin for the organic matter that, when mature, might produce gas products. This results trend agreed with previous study conducted on selected coal samples from Benue Trough basin [20].

According to Hunt [80], the petroleum potential of particular macerals increases with rising hydrogen-to-carbon (H/C) atomic ratios. By performing elemental analysis on kerogens or asphaltene, the H/C ratio is commonly determined [81]. The four varieties of kerogen—Type I, Type II, Type III, and Type IV—are distinguished by the ratios of H/C and O/C [82-84]. Type I is an aliphatic kerogen with initial H/C ratios that are high (>1.5) and low (0.1). Compared to Type I, Type II has a lower H/C ratio (roughly 1.0 to 1.4) and a more comprehensive range of O/C ratios (0.05-0.15). Due to land-dwelling plants, Type III Kerogen has low H/C ratios (0.6–0.9) and O/C ratios, typically between 0.1 and 0.3.

Despite having comparable O/C ratios > 0, type IV kerogen has the least amount of aliphatic-based kerogen and the least H/C (0.6). The organic matter with inertinite-rich macerals is found in type IV. The coals' H/C levels indicate the presence of Type III/IV organic materials. The Type IV kerogen inertinites comprise around 54% of GMG and are abundant. The coals under study are Type II organic matter (BMK), Type III organic matter (DDG, SKJ, OGB, AFZ, and WKP), and the boundary between Type III and Type IV organic matter (GMG), according to Figure 17. The GMG, WKP, DDG, and OG coals can generate gas when thermally matured (Fig. 18). BMK coal is rich in liptinite maceral and could potentially produce crude oils if thermally matured. AFZ and SKJ coals can produce mixed liquid hydrocarbons if subjected to sufficient thermal maturation.

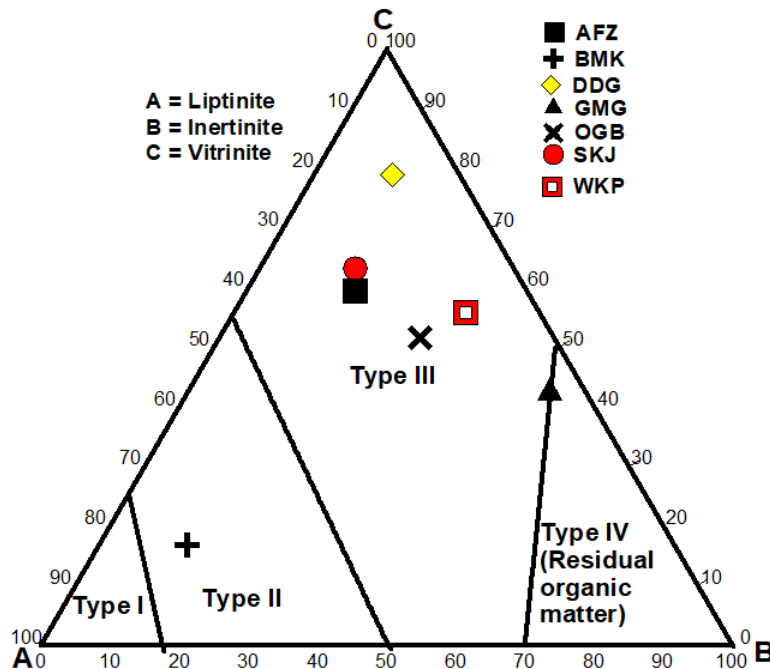


Fig. 17. Ternary plot of classification of kerogen type based on major organic components (modified after [85]).

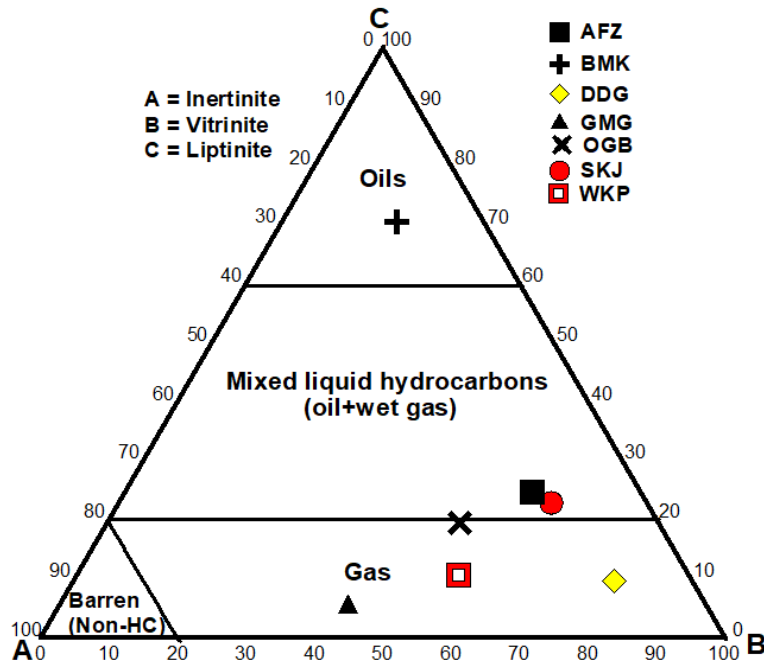


Fig. 18. Ternary diagram based on maceral composition indicating the hydrocarbon potential of coals of Benue Trough (adapted from [84]).

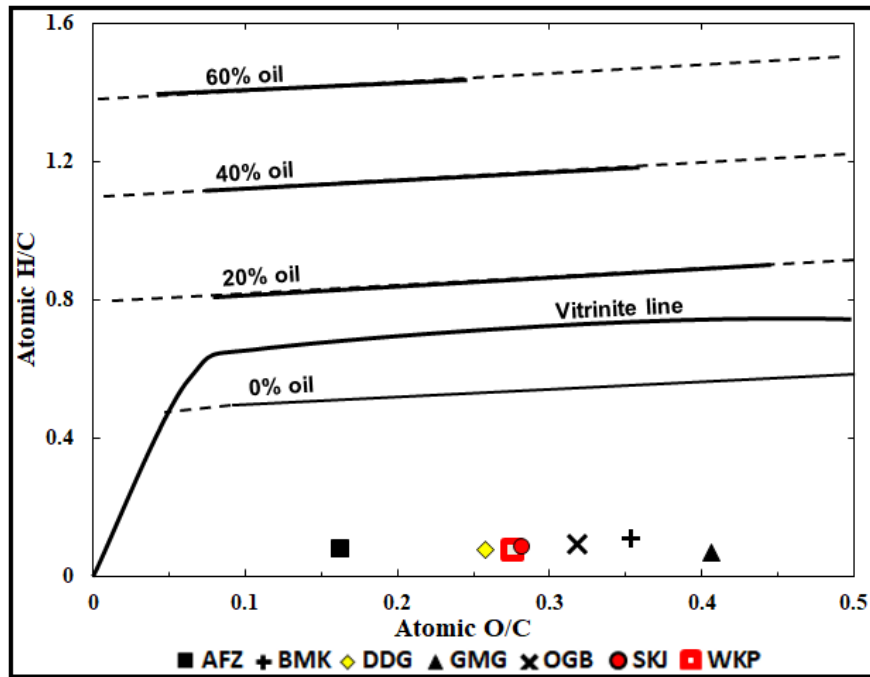


Fig. 19. Atomic H/C vs. O/C plots of vitrinite maturation line and calculated oil yields for slow pyrolysis (adapted from [86]).

All analysed coal samples are located below the oil generation zone in the plot, according to the elemental atomic ratio cross-plot in Figure 19. This finding supports the theory that coals can only emit gaseous hydrocarbons when matured. Numerous studies [82,87-90], have focused on the crucial importance of liptinites in evaluating the prospects of oil generation from coal. The literature reports numerous attempts to determine the lowest level of liptinite (exinite in vol.%) found in coal for oil generation [4,88,91]. Hunt [4] and Snowdon [88] both reported "15-20% liptinite + resinite," whereas [91] observed "a minimum of 15-20% liptinite."

Mukhopadhyay [90] stated that about 20–25% liptinite is needed to produce more than 10% pyrolysate. Thus, during the natural coalification process, liptinites and per-hydrous vitrinites may produce liquid hydrocarbons [2]. The varied compositions of perhydrous vitrinite are typically linked to the high liptinite content in humic-based coals [92–94]. Liptinite maceral groups in the investigated coal samples can range from 5.2% to 53.2%, indicating low to moderately high hydrogen-rich coals with the potential to produce gaseous and oil hydrocarbons.

A condensed version of Seyler's coal chart for the coals analyzed in this study is shown in Figure 20. Usually, the figure shows the relationship between H% and C% (in a dry, mineral-free base) along with overlaps that show how other thermochemical parameters fluctuate depending on the main variables. According to rank, the H% range for the ortho-hydrous bituminous coal class is shown as a band with values between 4.4 and 5.6. According to Seyler's chart, the hydrogen-rich coals plotted above this band are referred to as per-hydrous, while the hydrogen-poor coals plotted below the band are sub-hydrous. In Figure 20, the DDG and OGB coals exist in the sub-hydrous zone, while BMK and WKP are outside the parametric zones. The AFZ and SKJ coals are plotted in the per-hydrous zone.

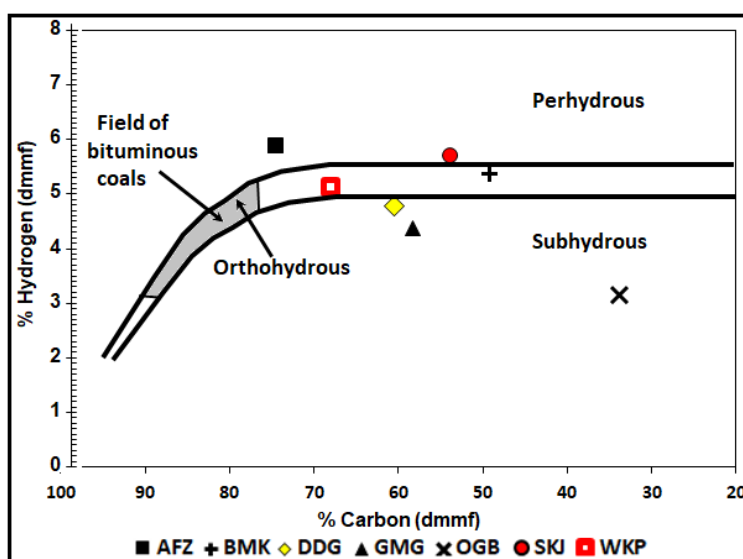


Fig. 20. Simplified Seyler chart showing the compositional fields of orthohydrous, perhydrous, and sub-hydrous coals, after Diessel [69].

4.6. Maturity

Vitrinite reflectance is a measure of the degree of light reflected by vitrinite, which is an organic rock component [95–96]. It is a measurement of maturity even if determined by the kerogen type [97]. The maturation threshold for coals to produce oil has been assigned as the vitrinite reflectance range of 0.5 - 0.6% Ro to 1.30 - 1.35% Ro ([4]). The early oil window stage (0.6 - 0.7%), early middle oil window (0.7 - 0.75%), middle oil window stage (0.75 - 0.9%), early upper oil window stage (0.9–1.0%), and upper oil window stage (1.0 - 1.3%) can all be further classified. Except for the early oil window thermal maturity stage (which ranges from 0.6 - 0.7% Ro) for DDG (0.63% Ro), OGB, and WKP (both at 0.55% and 0.53% Ro, respectively), all samples' measured Ro values (i.e., 0.44 - 0.63% Ro) indicate that the coals are immature to moderately mature. It is implied that the coals are immature because the maturation threshold is for vitric coals. Miles [81] also noted that the atomic ratio of H/C indicates a lack of maturity for Type III organic matter at values below 0.9.

All investigated coals have H/C ratios (0.07 - 0.11) below 0.9, making them thermally immature to barely mature. Particularly in predominately anaerobic environments, the deposition of organic matter in sedimentary paleoenvironments results in hydrogen enrichment [98–101]. Figure 21 shows the coals plotted beneath Kerogen Type III organic matter, whereas bituminous coals reflect the catagenetic period during which AFZ was first developed. Since the

outlined parameters remain constant despite the effects of diagenetic and in-reservoir alterations, the ratios of transition metals in crude oils are advantageous to the source rocks, depositional environment, and maturation assessment [9-11].

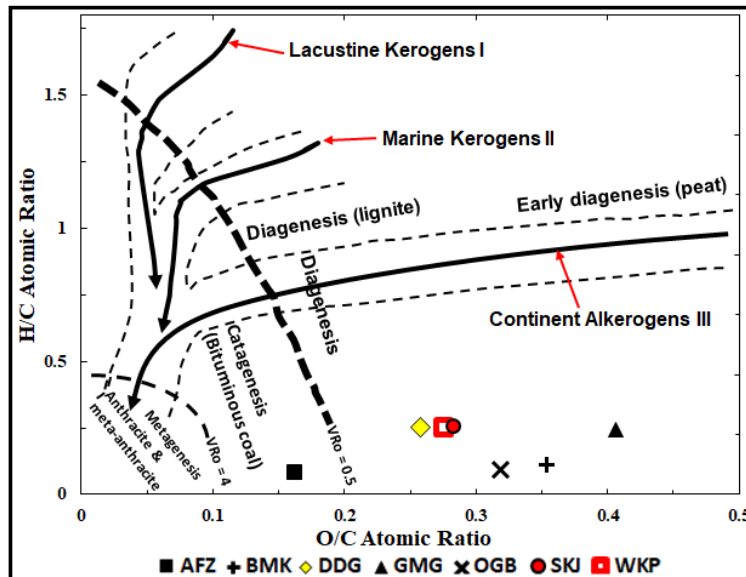


Fig. 21. The van Krevelen [102] diagram of O/C versus H/C (from Singh [103]) applied to the coals in the Benue Trough.

5. Conclusions

To comprehend coal quality and paleoenvironmental deposition, field observation and laboratory analytical methods were utilized to examine coal samples from numerous recently discovered coal seams in the Benue Trough Basin of Nigeria. The common minerals found in coals include kaolinite, quartz, feldspar, hematite, magnetite, calcite, siderite, dolomite, orthoclase, graphite, and illite (unknown crystal plane). Coal samples experienced weight loss due to moisture loss, volatile matter loss, and fixed carbon combustion. High volatile matter yield, average low ash yield, average high fixed carbon, and average low sulphur values indicated an excellent coal grade. Most organic matter is vitrinite, which accounts for an average volume percentage of 52.63% (free of minerals). All tested coal samples have varying quantities of inertinite and liptinite. The Obomkpa (BMK) sample had the highest content of liptinite. The coal samples were collected in an area of the moor that varied between anoxic and oxic environments. Coal samples from DDG and SKJ were placed in planar central mires that frequently flood.

In contrast, a flat border marsh that had briefly been submerged was where OGB and BMK were discovered. In transitional dry mire and transitional-wet mires, respectively, the GMG and WKP coals were laid down. In AFZ, BMK, DDG, OGB, WKP, and SKJ, high-GI, and low-TPI coals were discovered. These coals were laid down in limno-telmatic facies—moist woodland swamps—where organic materials accumulated quickly. Given that GMG has a high TPI and a low GI, it may be assumed that terrestrial plants (plant fossils) contribute significantly to the development of mire-based processes of decay and degradation of wood (i.e. maceral development).

Acknowledgements

The Tertiary Education Trust Fund (TET-Fund) of Nigeria provided a research grant, which is warmly welcomed.

Funding: The present study was funded by Tertiary Education Trust Fund (TET-Fund) of Nigeria.

Availability of data and material (data transparency): All the data generated during the course of the present study are included in this manuscript.

Conflicts of Interest /Competing interests: There is no conflict of interest among the authors themselves or between the authors and the funder (TET-FUND, Nigeria).

Authors' contributions: All authors contributed to the study's conception and design.

Project planning and execution and entire experimental work: Segun A. Akinyemi; Ayobami T. Kayode; Olajide F. Adebayo. Writing - Manuscript preparation, review and editing: Segun A. Akinyemi; Ayobami T. Kayode; Henry Y. Madukwe; Bemgba B. Nyakuma; James C. Hower. Petrographic analysis and write up: James C. Hower; Segun A. Akinyemi. Mineralogic analysis and write up: Abiodun B. Ogbesejana; Binoy K. Saikia. Funding acquisition: Segun A. Akinyemi; Olajide F. Adebayo.

All the eleven authors have read and approved the final manuscript.

References

- [1] Diessel C. An appraisal of coal facies based on maceral characteristics. *Australian Coal Geology* 1982; 4(2): 474-484.
- [2] Wilkins RW, George SC. Coal as a source rock for oil: a review. *International Journal of Coal Geology* 2002; 50(1-4): 317-361.
- [3] Bertrand P, Behar F, Durand B. Composition of potential oil from humic coals in relation to their petrographic nature. *Organic Geochemistry* 1986; 10(1-3): 601-608.
- [4] Hunt JM. Generation of gas and oil from coal and other terrestrial organic matter. *Organic Geochemistry* 1991; 17(6): 673-680.
- [5] Hutton A, Daulay B, Nas C, Pujobroto A, Sutarwan H. Liptinite in Indonesian tertiary coals. *Energy & Fuels* 1994; 8(6): 1469-1477.
- [6] Boreham C, Blevin J, Radlinski A, Trigg K. Coal as a source of oil and gas: a case study from the Bass Basin, Australia. *The Australian Petroleum Production and Exploration Association Journal* 2003; 43(1): 117-148.
- [7] Kotarba M J, Clayton JL, Rice DD, Wagner M. Assessment of hydrocarbon source rock potential of Polish bituminous coals and carbonaceous shales. *Chemical Geology*, 2002; 184(1-2): 11-35.
- [8] Bechtel A, Gruber W, Sachsenhofer R, Gratzner R, Püttmann W. Organic geochemical and stable carbon isotopic investigation of coals formed in low-lying and raised mires within the Eastern Alps (Austria). *Organic geochemistry* 2001; 32(11): 1289-1310.
- [9] Udo O. Some trace metal in selected Niger Delta crude oils: application in oil-oil correlation studies. *Journal of Mining and Geology* 1992; 28(2): 289-291.
- [10] Barwise AJG. Role of nickel and vanadium in petroleum classification. *Energy and Fuels* 1990; 4: 647-652.
- [11] Lewan MD. Factors controlling the proportionality of vanadium to nickel in crude oils. *Geochimica et Cosmochimica Acta* 1984; 48(11): 2231-2238.
- [12] Ekweozor CM, Unomah GI. First discovery of oil shale in the Benue Trough, Nigeria *Fuel* 1990; 69: 502-508.
- [13] Jauro A, Obaje NG, Agho MO, Abubakar MB, Tukur A. Organic geochemistry of Cretaceous Lamza and Chikila coals, upper Benue Trough, Nigeria. *Fuel* 2007; 86: 520 – 532.
- [14] Abubakar MB. Petroleum Potentials of the Nigerian Benue Trough and Anambra Basin: A Regional Synthesis. *Natural Resources* 2014; 5: 25-58 pp. DOI:10.4236/nr.2014.51005
- [15] Ohimain EI. Can Nigeria generate 30% of her electricity from coal? *International Journal of Energy and Power Engineering* 2014; 3: 28-37.
- [16] Raji JK, Adebawale AOJ. Petroleum Source Rock Potential of the Upper Benue Trough, Nigeria: Implications for Hydrocarbon Exploration. *Society of Petroleum Engineers*. 2015. doi:10.2118/178348-MS.
- [17] Nyakuma B, Jauro A, Oladokun O, Bello A, Alkali H, Modibo M, Abba M. Physicochemical, Mineralogical, and Thermogravimetric Properties of Newly Discovered Nigerian Coals. *Petroleum & Coal* 2018; 60: 641-649.
- [18] Akinyemi SA, Adebayo OF, Nyakuma BB, Adegoke AK, Aturamu OA, OlaOlorun O A, Adetunji A, Hower JC, Hood MM, Jauro A. Petrology, physicochemical and thermal analyses of selected cretaceous coals from the Benue Trough Basin in Nigeria. *Int J Coal Sci Technol*. 2020; 7(1): 26-42.
- [19] Akinyemi, S. A., Nyakuma, B. B., Jauro, A., Adebayo, O. F., OlaOlorun, O. A., Adegoke, A. K., Aturamu, A. O., Adetunji, A., Gitari, M. W., Mudzielwana, R., Mineralogy, physicochemical

- and oxidative thermal analyses of Cretaceous coals from the Benue Trough, Nigeria. *Energy Geoscience* 2021; 2: 129 - 135.
- [20] Akinyemi SA, Adebayo OF, Madukwe HY, Kayode AT, Aturamu, AO, OlaOlorun OA, Nyakuma, BB, Jauro A, Gitari WM, Mudzielwana R, Hower JC. Elemental Geochemistry and Organic Facies of Selected Cretaceous Coals from the Benue Trough basin in Nigeria: Implication for Paleodepositional Environments. *Marine and Petroleum Geology* 2022; 137: 105490.
- [21] Obaje NG, Ligous B, Abaa SI. Petrographic composition and depositional environments of Cretaceous coals and coal measures in the middle Benue Trough of Nigeria. *Int J Coal Geol.* 1994; 26: 233-60.
- [22] Ogala J, Siavalas G, Christanis K. Coal petrography, mineralogy and geochemistry of lignite samples from the Ogwashi-Asaba Formation, Nigeria. *Journal of African Earth Sciences* 2012; 66-67: 35 - 45.
- [23] Mangs AD, Wagner NJ, Moroeng OM, Lar UA. Petrographic composition of coal within the Benue Trough, Nigeria and a consideration of the paleodepositional setting. *International Journal of Coal Science & Technology* 2022; 9: 35.
- [24] Fatoye FB, Gideon YB. Geology and occurrences of limestone and marble in Nigeria. *Journal of Natural Sciences Research* 2013; 3(11): 60-65.
- [25] Benkheilil J. The origin and evolution of the Cretaceous Benue Trough (Nigeria). *Journal of African Earth Sciences (and the Middle East)* 1989; 8(2-4): 251-282.
- [26] Petters SW. Central West African Cretaceous-Tertiary benthic foraminifera and stratigraphy. *Palaeontographica Abteilung A* 1982; 1-104.
- [27] Obaje N, Abaa S, Najime T, Suh C. Economic geology of Nigerian coal resources brief review. *Africa Geoscience Review* 1999; 6: 71-82.
- [28] Olade M. Evolution of Nigeria's Benue Trough (Aulacogen): a tectonic model. *Geological Magazine* 1975; 112(6): 575-583.
- [29] Nwajide C. Cretaceous sedimentation and palaeogeography of the central Benue Trough. *The Benue. Tough Structure and Evolution International Monograph Series, Braunschweig* 1990; 19-38.
- [30] Idowu J, Ekweozor, C. Petroleum potential of Cretaceous shales in the Upper Benue Trough, Nigeria. *Journal of Petroleum Geology* 1993; 16(3): 249-264.
- [31] Uzuakpunwa A. The Abakaliki pyroclastics, Eastern Nigeria: new age and tectonic implications. *Geological Magazine* 1974; 111(1): 65-70.
- [32] Ojoh K. The southern part of the Benue Trough (Nigeria) Cretaceous stratigraphy, basin analysis, paleo-oceanography and geodynamic evolution in the Equatorial domain of the South Atlantic. *NAPE Bulletin* 1992; 7: 67-74.
- [33] Murat R. Stratigraphy and palaeogeography of the Cretaceous and Lower Tertiary in southern Nigeria. *African Geology* 1972; 1(1): 251-266.
- [34] Reyment RA. Aspects of the geology of Nigeria—The Stratigraphy of the Cretaceous and Cenozoic Deposits. Ibadan University Press 1965; 133 p.
- [35] Nwachukwu S. The tectonic evolution of the southern portion of the Benue Trough, Nigeria. *Geological Magazine* 1972; 109(5): 411-419.
- [36] Akinniyi A, Ola S. Investigation of certain engineering properties of some Nigerian limestone deposits for cement production. *Electronic Journal of Geotechnical Engineering* 2016; 21: 10471-10482.
- [37] Fatoye FB, Gideon, YB. Appraisal of the economic geology of Nigerian coal resources. *Journal of Environment and Earth Science* 2013; 3(11): 25-31.
- [38] Obaje NG. Geology and mineral resources of Nigeria. *Lecture Notes in Earth Sciences* 2009; 120: 221.
- [39] Miller BG. Clean Coal Engineering Technology. *Technology & Engineering* 2016; 2: 856.
- [40] Speight JG. The Chemistry and Technology of Coal. Chemical Industries. 2012; 8.
- [41] ASTM D2013/D2013M-12. Standard Practice for preparing coal samples for analysis. West Conshohocken, PA, USA: ASTM International 2012.
- [42] ASTM D7582-12, Standard Test Methods for Proximate Analysis of Coal and Coke by Macro Thermogravimetric Analysis, ASTM International, West Conshohocken, PA. 2012. www.astm.org
- [43] Standard, A. D4239-12. Test Method for Sulfur in the Analysis Sample of Coal and Coke Using High-Temperature Tube Furnace Combustion. ASTM International, West Conshohocken, PA, 2012.
- [44] ASTM D3176-15. Standard Practice for Ultimate Analysis of Coal and Coke, Barwise, A. Role of nickel and vanadium in petroleum classification. *Energy & Fuels* 1990; 4(6), 647-652.

- [45] ISO 7404-2. Methods for the petrographic analysis of coals — Part 2: Methods of preparing coal samples. 2009.
- [46] ASTM D7708-14, Standard Test Method for Microscopical Determination of the Reflectance of Vitrinite Dispersed in Sedimentary Rocks, ASTM International, West Conshohocken, PA, 2014, www.astm.org
- [47] Pickel W, Kus J, Flores D, Kalaitzidis S, Christanis K, Cardott BJ, Misz-Kennan M, Rodrigues S, Hentschel A, Hamor-Vido M, Crosdale P, Wagner N, ICCP. Classification of liptinite-ICCP System 1994. *Int. J. Coal Geol.* 2017; 169: 40–61.
- [48] ICCP., The new vitrinite classification (ICCP System 1994). *Fuel* 1998; 77(5): 349-358.
- [49] ICCP., The new inertinite classification (ICCP System 1994). *Fuel* 2001; 80(4): 459-471.
- [50] Sýkorová I, Pickel W, Christanis K, Wolf M, Taylor GH, Flores D. Classification of huminite - ICCP System 1994. *International Journal of Coal Geology* 2005; 62: 85-106.
- [51] ISO 7404-5. Methods for the petrographic analysis of coals — Part 5: Method of determining microscopically the reflectance of vitrinite. 2009.
- [52] Saikia BK, Boruah RK, Gogoi PK. FT-IR and XRD analysis of coal from Makum coalfield of Assam. *Journal of Earth System Science* 2007; 116(6): 575-9.
- [53] Singh MP, Singh PK. Petrographic characterization and evolution of the Permian coal deposits of the Rajmahal basin, Bihar, India. *International Journal of Coal Geology* 1996; 29(1-3): 93-118.
- [54] Singh M. P, Singh AK. Petrographic characteristics and depositional conditions of Eocene coals of platform basins, Meghalaya, India. *International Journal of Coal Geology* 2000; 42(4): 315-356.
- [55] Misiak, J., 2002. Środowiska depozycji materii organicznej w torfowiskach karbońskich. Materiały XXV Sympozjum „Geologia formacji węglonośnych Polski”, AGH, Kraków 2002; 105-108.
- [56] Misiak J. Petrography and depositional environment of the No. 308 coal seam (Upper Silesian Coal Basin, Poland) - a new approach to maceral quantification and facies analysis. *International Journal of Coal Geology* 2006; 68(1-2): 117-126.
- [57] Ward CR. Analysis and significance of mineral matter in coal seams. *International Journal of Coal Geology* 2002; 50(1-4): 135-168.
- [58] Misiak J. Projekt diagramu do analizy facjalnej pokładów węgla kamiennego. *Mat. XXIV Symp. nt. Geologia formacji węglonośnych Polski* 2003.
- [59] Mastalerz M, Padgett PL, Eble CF. Block coals from Indiana: inferences on changing depositional environment. *International Journal of Coal Geology* 2000; 43(1-4): 211-226.
- [60] Warbrooke PR. Depositional and chemical environments in Permian coal forming swamps from the Newcastle area. In *The Twenty Eighth Newcastle Symposium on Advances in the Study of the Sydney Basin* 1987; 1-9.
- [61] O’Keefe JMK, Bechtel A, Christanis K, Dai S, DiMichele WA, Eble CF, Esterle JS, Mastalerz M, Raymond AL, Valentim BV, Wagner, NJ, Ward CR, Hower JC. On the fundamental difference between coal rank and coal type. *Int. J. Coal Geology* 2013; 118: 58-87.
- [62] Diessel C. On the correlation between coal facies and depositional environments. in *Proceeding 20th Symposium of Department Geology, University of New Castle, New South Wales.* 1986.
- [63] Dai S, Bechtel A, Eble CF., Flores, R.M., French, D., Graham, I.T., Hood, M.M., Hower JC, Korasidis VA, Moore TA, Püttmann W, Wei Q, O’Keefe JMK. Recognition of peat depositional environments in coal: A review. *Int. J. Coal Geology* 2020; 219: 103383, <https://doi.org/10.1016/j.coal.2019.103383>.
- [64] Calder JH, Gibling MR, Mukhopadhyay PK. Peat formation in a Westphalian B piedmont setting, Cumberland Basin, Nova Scotia; implications for the maceral-based interpretation of rheotrophic and raised paleomires. *Bulletin de la Société Géologique de France* 1991;162(2): 283-298.
- [65] Flores D. Organic facies and depositional palaeoenvironment of lignites from Rio Maior Basin (Portugal). *International Journal of Coal Geology* 2002; 48(3-4): 181-195.
- [66] Teichmüller M. The genesis of coal from the viewpoint of coal petrology. *International Journal of Coal Geology* 1989; 12(1-4): 1-87.
- [67] Teichmuller M, Teichmuller R. *Stach’s textbook of coal petrology.* Gebruder Borntraeger, Berlin, Stuttgart. 1982.
- [68] Hower JC, Eble CF, O’Keefe JMK. Phyteral perspectives: Every maceral tells a story. *Int. J. Coal Geol.* 2021; 247: 103849.
- [69] Diessel CF.) *Coal-bearing depositional systems.* Springer Science & Business Media 2012.

- [70] Alves R, Ade M. Sequence stratigraphy and coal petrography applied to the Candiota Coal Field, Rio Grande do Sul, Brazil: A depositional model. *International Journal of Coal Geology* 1996; 30(3): 231-248.
- [71] Gómez Neita JS, López Carrasquilla MD. Paleoenvironments of coals using organic petrography and their relationship with physicochemical properties, Guaduas formation, Checua-Lenguaque syncline. (Trabajo de grado). Universidad Pedagógica y Tecnológica de Colombia, Sogamoso 2017. <http://repositorio.uptc.edu.co/handle/001/1875>
- [72] Prahlg FG, Bennett JT, Carpenter R. The early diagenesis of aliphatic hydrocarbons and organic matter in sedimentary particulates from Dabob Bay, Washington. *Geochimica et Cosmochimica Acta* 1980; 44(12): 1967-1976.
- [73] Premuzic ET, Benkovitz CM, Gaffney JS, Walsh JJ. The nature and distribution of organic matter in the surface sediments of world oceans and seas. *Organic Geochemistry* 1982; 4(2): 63-77.
- [74] Prahlg FG, Ertel JR, Goñi MA, Sparrow MA, Eversmeyer B. Terrestrial organic carbon contributions to sediments on the Washington margin. *Geochimica et Cosmochimica Acta* 1994; 58(14): 3035-3048.
- [75] Jasper JP, Gagosian RB. The sources and deposition of organic matter in the Late Quaternary Pigmy Basin, Gulf of Mexico. *Geochimica et Cosmochimica Acta* 1990; 54(4): 1117-1132.
- [76] Ishiwatari R, Uzaki M. Diagenetic changes of lignin compounds in a more than 0.6 million-year-old lacustrine sediment (Lake Biwa, Japan). *Geochimica et Cosmochimica Acta* 1987; 51(2), 321-328.
- [77] Meyers PA, Ishiwatari R. Lacustrine organic geochemistry-an overview of indicators of organic matter sources and diagenesis in lake sediments. *Organic Geochemistry* 1993; 20(7): 867-900.
- [78] Meyers PA. Preservation of elemental and isotopic source identification of sedimentary organic matter. *Chemical geology*, (1994). 114(3-4), 289-302.
- [79] Pelet R. Preservation and alteration of present-day sedimentary organic matter. *Advances in Organic Geochemistry* 1981; 198(1): 24.
- [80] Hunt JM. *Petroleum geochemistry and geology*. W. H. H. Freeman and Co.: San Francisco 1979; 483.
- [81] Miles JA. *Illustrated glossary of petroleum geochemistry*. Oxford, Clarendon Press. 1989; 137p.
- [82] Tissot, B., Welte, D., *Petroleum formation and occurrence*. Springer-Verlag, New York 1978; 538.
- [83] Durand B, Monin, J. Elemental analysis of kerogens (C, H, O, N, S, Fe), in *Kerogen*. 1980; Editions Technip Paris 1980; 113-142.
- [84] Tissot B, Welte D. 1984. *Petroleum Formation and Occurrence*, 2nd edn 1980; 699 pp.
- [85] Cornford C. Organic deposition at a continental rise: organic geochemical interpretation and synthesis at DSDP Site 397, eastern North Atlantic. von Rad, U., Ryan, WBF, et al., *Init. Repts. DSDP* 1979; 47: 503-510.
- [86] Saxby JD. Atomic HC ratios and the generation of oil from coals and kerogens. *Fuel* 1980; 59(5): 305-307.
- [87] Horsfield B, Yordy K, Crelling J. Determining the petroleum-generating potential of coal using organic geochemistry and organic petrology. *Organic Geochemistry in Petroleum Exploration* 1988; 121-129.
- [88] Snowdon LR. Oil from type III organic matter: resinite revisited. *Organic Geochemistry*, 1991; 17(6): 743-747.
- [89] Hendrix, M. S., Brassell, S. C., Carroll, A. R., Graham, S. A., *Sedimentology, organic geochemistry, and petroleum potential of Jurassic coal measures: Tarim, Junggar, and Turpan basins, Northwest China*. AAPG Bulletin 1995; 79(7): 929-958.
- [90] Mukhopadhyay P, Hatcher P, Calder J. Hydrocarbon generation from deltaic and intermontane fluviodeltaic coal and coaly shale from the Tertiary of Texas and Carboniferous of Nova Scotia. *Organic Geochemistry* 1991; 17(6): 765-783.
- [91] Mukhopadhyay PK, Hatcher PG. Composition of Coal, in *Hydrocarbons from coal*, in Law, BaR, DD, eds.. Editor. 1993; American Association of Petroleum Geologists Studies in Geology: USA 1993; 79-118.
- [92] Price LC, Baker CE. Suppression of vitrinite reflectance in amorphous rich kerogen-a major unrecognized problem. *Journal of Petroleum Geology* 1985; 8(1): 59-84.
- [93] Kalkreuth W. Rank and petrographic composition of selected Jurassic-Lower Cretaceous coals of British Columbia, Canada. *Bulletin of Canadian Petroleum Geology* 1982; 30(2): 112-139.

- [94] Raymond AC, Murchison DG. Influence of exinitic macerals on the reflectance of vitrinite in Carboniferous sediments of the Midland Valley of Scotland. *Fuel* 1991; 70(2): 155-161.
- [95] Barker CE, Pawlewicz MJ. An empirical determination of the minimum number of measurements needed to estimate the mean random vitrinite reflectance of disseminated organic matter: *Organic Geochemistry* 1993; 20(6): 643-651.
- [96] Hackley, P. C., Cardott, B. J. 2016. Application of organic petrography in North American shale petroleum systems: A review. *International Journal of Coal Geology* 163, 8-51.
- [97] Peters KE, Moldowan JM. *The biomarker guide: interpreting molecular fossils in petroleum and ancient sediments*. 1993.
- [98] Newman J, Newman N. Reflectance anomalies in Pike River coals: evidence of variability in vitrinite type, with implications for maturation studies and "Suggate rank". *New Zealand Journal of Geology and Geophysics* 1982; 25(2): 233-243.
- [99] Gentzis T, Goodarzi F. Reflectance suppression in some Cretaceous coals from Alberta, 601 Canada. *ACS Symposium Series* 1994; 570: 93-110.
- [100] Gurba LW, Ward CR. Vitrinite reflectance anomalies in the high-volatile bituminous coals of the Gunnedah Basin, New South Wales, Australia. *International Journal of Coal Geology* 1998; 36(1-2): 111-140.
- [101] Petersen H, Rosenberg P. Reflectance retardation (suppression) and source rock properties related to hydrogen-enriched vitrinite in Middle Jurassic coals, Danish North Sea. *Journal of Petroleum Geology* 1998; 21(3): 247-263.
- [102] van Krevelen DW. *Coal--typology, chemistry, physics, constitution*. 1961; 3.
- [103] Singh PK, Singh M, Singh AK, Naik A. Petrographic and geochemical characterization of coals from Tiru valley, Nagaland, NE India. *Energy Exploration & Exploitation* 2012; 30(2): 171-191.

*To whom correspondence should be addressed: Dr. Bemgba B. Nyakuma, ³Department of Chemical Sciences, Faculty of Science and Computing, North-Eastern University Gombe, P.M.B. 0198 Gombe State, Nigeria, E-mail: bemgba.nyakuma@neu.edu.ng et bbnyax1@gmail.com
<https://orcid.org/0000-0001-5388-7950>*